T H E U N I V E R S I T Y O F M I C H I G A N

COLLEGE OF ENGINEERING
Department of Civil Engineering

Final Report

THE MECHANICS OF SURFACE DEFORMATION AND RESISTANCE TO A SPHERE ROLLING DOWN SLOPES OF GRANULAR MEDIA

Y. K. Lin
R. Haythornthwaite

ORA Project 05894

under contract with:

U. S. ARMY-TANK AUTOMOTIVE COMMAND
CONTRACT NO. DA-20-018-AMC-0980T
WARREN, MICHIGAN

administered through:

OFFICE OF RESEARCH ADMINISTRATION ANN ARBOR

January 1969

TABLE OF CONTENTS

LIST OF ILLUSTRATIONS

ABSTRACT

A simple theory is proposed which describes the mechanics of a sphere rolling down a slope of cohesionless, granular material at constant velocity. The theory is based on a "bulldozing action" by the rolling sphere and a "flotation or buoyancy" effect from material displaced by the sphere.

A dimensional analysis of the problem was carried out from which a functional relationship was established between the shear strength properties of the granular material, the sphere density, bed density, and depth of groove or track left by the rolling sphere. This relationship was tested experimentally for both a well-rounded, medium grained Ottawa sand, and a crushed, Turkish emery. The latter was much more angular and possessed a higher specific gravity.

The theoretical prediction was quite good for the Ottawa sand and somewhat less satisfactory for the Turkish emery. In the latter case the deviation and scatter of test results was likely due to experimental difficulty in measuring the depth of track because of grain angularity and particle orientation.

In view of the simplifying assumptions made, the theory appears to describe quite well the mechanics of a sphere rolling down a inclined bed of granular media. With additional refinements the theory could be usefully applied to terrestrial vehicle mobility problems and to prediction of lunar surface properties from observation and remote measurement of lunar boulder tracks.

INTRODUCTION

In many vehicle mobility or land locomotion problems it is desirable to obtain a general relationship between the surface properties of the ground on which a vehicle travels and the deformation of the surface. The mechanics of a sphere rolling down a slope of cohesionless, granular material at constant velocity is a special case in point. A theoretical analysis was derived to describe this case based on the "bulldozing" action of a rolling sphere and on the "buoyancy or flotation" effect from material displaced by the sphere. This relationship was tested experimentally for two types of soil or granular material.

The objectives of the study were twofold: to improve our fundamental understanding of vehicle mobility or land locomotion problems and to develop prediction criteria for estimating surface shear strength of granular soils from observation and measurement of tracks left by a rolling object. The latter objective has particular significance in regard to prediction of lunar soil properties from limited information presently available to us.

An analysis of vehicle performance may be subdivided[1] into two groups—a study of stability problems on the one hand, and elasticity problems on the other. The former deals with conditions for equilibrium immediately preceding ultimate failure by plastic flow, the latter with deformations of a soil due to its own weight or due to external forces such as the weight of a vehicle. Elastic theory is limited to very small deformations, e.g., pavement deflections under a wheel load; consequently, it is not universally applicable to all vehicle mobility problems. Consider the case of a vehicle moving cross country: in this instance we can expect large surface deformations, especially in soft ground or loose, cohesionless soil. Under these conditions plastic flow will result, and a plasticity analysis would be more suitable. The problem of a dense sphere rolling down a bed of cohesionless, granular material falls into this category.

The analysis described herein is potentially useful for prediction of lunar soil properties from observation of boulder tracks on the moon's surface. Sightings and measurement of tracks left by boulders or rock fragments on the moon's surface have been reported frequently, e.g., Surveyor II, V and Orbiter II and V lunar missions. In order to use the track information to predict the shear strength or bearing capacity of lunar soils it is necessary to know something about the composition (density) of the lunar surface or vice versa. The latest concensus[3] in this regard is that the lunar surface is composed of a material similar to a plateau basalt. Suggestions as to the mechanical properties of lunar soils, such as particle shape, size, porosity internal friction, cohesion, and sensitivity also have been reported in the literature.[2,4]

THEORETICAL ANALYSIS

The mechanics of a rigid sphere rolling down an inclined bed of deformable material e.g., a cohesionless sand, will be somewhat different than that of a rigid sphere rolling down an inclined surface of a rigid, nonyielding material. The advancing force in the latter case depends on the weight of the sphere, the inertial force due to sphere motion, and the friction force between the sphere and the inclined surface. On the other hand, when the sphere rolls down on inclined bed of deformable material some sinkage will occur, a groove will be formed, and the advancing force available to overcome internal resistance in the material will be reduced because of a buoyancy effect. Accordingly, the effective weight of the sphere may be considered as the weight of the sphere, W, less the weight, w, of granular material displaced by the portion of the sphere lying below the original surface.

For simplicity, the analysis is based on the following restrictions or boundary conditions:

1. The sphere rolls down at constant velocity.
2. The inclined surface possesses constant slope.
3. There is no slip between the sphere and the inclined surface.

A sphere lying on a horizontal surface of granular media will indent to some degree, but rolling will not occur. For a certain slope, the sphere will start rolling. Assume rolling is essentially a "bulldozing" action in which the granular material is pushed forwards, upwards and sideways by the moving sphere. The state of motion is complicated and the stress distribution is indeterminate. However, the material immediately ahead of the sphere might be expected to be forced to a stress state close to the passive Rankine state for the particular slope, and the x component, R, of the forces across the yz plane, as shown in Figure 1, could be related to the effective weight, W-w, and the slope angle, α. Accordingly, an equation of the following form can be written:

$$f(W-w,\ R,\ \alpha) = 0 \tag{1}$$

By virtue of Buckingham's theorem, this can be reduced to the form

$$f'\left[\frac{(W-w)\sin\alpha}{R}\right] = 0 \tag{2}$$

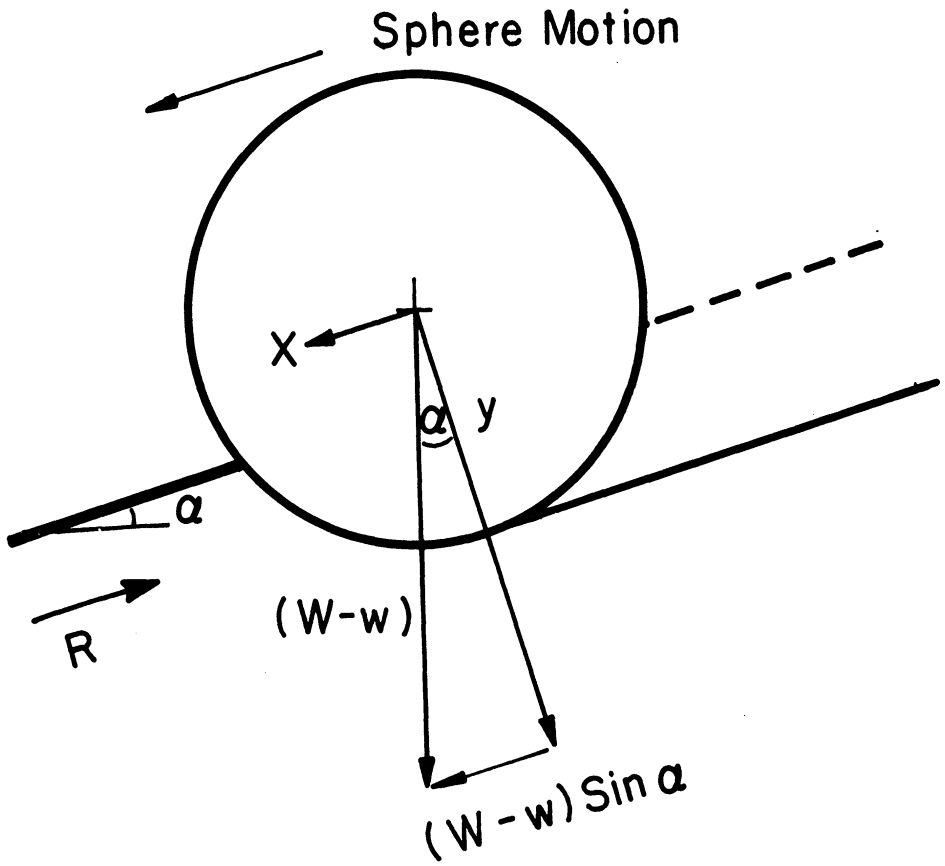

Figure 1. Diagram indicating local state of plastic equilibrium for ideal granular material.

It is important to note that the analysis has been restricted to the case which the sphere rolls down at constant speed. The slope of the inclined surface, α, is adjusted to satisfy the boundary condition of constant velocity; it is not an independent parameter. From initial experiments it was observed that the angle α is a linear function of the density of the sphere, γ_b, and the density of the granular media, γ_s. Therefore, a more general expression of the relation given in Eq. (1) can be written in the following manner,

$$g(W\text{-}w,\ R,\ \gamma_b,\ \gamma_s) = 0 \qquad (3)$$

The dimensional matrix of the variables is

	W-w	R	γ_b	γ_s
M	1	1	1	1
L	1	1	-2	-2
T	-2	-2	-2	-2

The rank of the matrix is 2, i.e., it contains a nonzero determinant of order 2 in its middle two columns, but does not contain a nonzero determinant of order larger than 2.

A product π^* of these variables with k_i exponents can be written in the following form:

$$\pi^* = (W-w)^{k_1} R^{k_2} \gamma_b^{k_3} \gamma_s^{k_4}$$

The homogeneous linear algebraic equations corresponding to the first two rows of the matrix are

$$\begin{aligned} k_1 + k_2 + k_3 + k_4 &= 0 \\ k_1 + k_2 - 2k_3 - 2k_4 &= 0 \end{aligned} \tag{4}$$

Since the number of the columns in the matrix is twice the rank of the matrix, the solution is not expected to be unique. One of the possible solutions may be

$$k_1 = 1,\ k_2 = -1,\ k_3 = 1/2,\ k_4 = -1/2.$$

Therefore, a possible product of these variables is

$$\pi^* = (W-w)^1 R^{-1} \gamma_b^{1/2} \gamma_s^{-1/2} \tag{5}$$

Buckingham's theorem states that $g(\pi^*) = 0$, whence $\pi^* = K_1$, a constant. It follows that

$$K_1 = \frac{W-w}{R}\left[\frac{\gamma_b}{\gamma_s}\right]^{1/2} \tag{6}$$

K_1 is probably dependent on the sinkage which is directly related to buoyancy action. The degree of sinkage can be considered as "flotation" depth at least in the case of relatively light spheres. The functional grouping $\frac{w}{W}$ might also be a significant variable. Examining the boundary conditions (Figure 2),

$$\text{at } \frac{w}{W} = 0,\ w = 0,\ \text{then } R = 0,\ K_1 \to \infty;$$

$$\text{at } \frac{w}{W} = 1,\ W-w = 0,\ K_1 = 0.$$

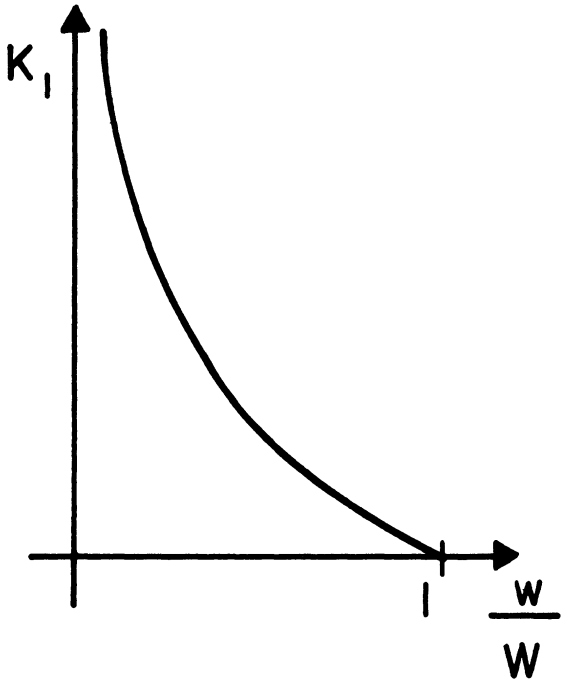

Figure 2. Relation between function K_1 and variable w/W.

In view of these conditions, a possible functional relation may be established as follows:

$$K_2 = \frac{w}{W}(K_1 + K_2) \tag{7}$$

Substituting (7) into (6), one obtains

$$K_2 = \frac{w}{R}\left[\frac{\gamma_b}{\gamma_s}\right]^{1/2} \tag{8}$$

Expressions for w and R are derived and given in Appendices II, and III, respectively. These two variables can be written as follows:

$$w = \frac{\pi}{4} r^3 \gamma_s \theta_o^4$$

$$R = \frac{1}{6} r^3 \gamma_s \theta_o^5 \left[\frac{1+\sin\phi}{1-\sin\phi}\right] \tag{9}$$

where r is the radius of the sphere, θ_o is the angle of half of the groove cross section measured at the center of the sphere, ϕ is the internal friction angle of the granular material. Substituting (9) into (8), one finally obtains

$$K_2 = \frac{\frac{3\pi}{2}\,\frac{1-\sin\phi}{1+\sin\phi}\left[\frac{\gamma_b}{\gamma_s}\right]^{1/2}}{\theta_o}$$

or

$$K = \frac{1-\sin\phi}{1+\sin\phi}\left[\frac{\gamma_b}{\gamma_s}\right]^{1/2}\theta_o^{-1} \qquad (10)$$

The values of K depend upon the properties of the granular media and the spheres. Accordingly, this relationship may be tested experimentally.

EXPERIMENTS

The experimental equipment consisted of four essential parts: a bin containing a bed of granular material, a device for depositing the material at a given void ratio, a velocity monitoring system, and spheres of various weights.

A bin of 117 cm long, 23 cm wide and 6.7 cm deep, with an adjustable incline angle, was built. A simple sand deposit device was made from a container suspended above the bin. The height of the container above the bin and the size of an opening in the bottom of the container could be regulated to change the rate of the sand flowing into the bin, thus varying the void ratio of the deposit. A row of photo cells and lights were mounted along the length of the bin. The photo cell circuit was so wired that it would be interrupted when one of the light beams was obscured by passage of a rolling sphere. The interruption was recorded automatically and the velocity of the rolling sphere ascertained by noting the spacing of interruptions on a recorder tracing. Figure 3 shows general view of the experimental set up.

The variation in specific gravity of the spheres was accomplished by drilling three holes of different sizes in bronze balls. The three holes were of equal diameter and were mutually perpendicular to assure isotropy of inertia. All spheres were encapsulated in table tennis balls for uniform surface properties. These bronze balls are shown in Figure 4.

The bin was laid horizontally during sand deposition. The height and opening of the deposit device was adjusted to obtain the various void ratios, e. The internal friction angle, ϕ, was then determined for each void ratio. The e- ϕ relation was obtained from triaxial tests on each material.

After sand deposition, the bin was tilted to a desired angle, and a sphere of a given density rolled down the inclined surface, as shown in Figure 5. The velocity of the rolling sphere was determined by monitoring the elapsed times between signals produced by the interruption of current when the sphere crossed a light beam. Only the results with constant velocity of the spheres were used in the experimental analyses.

The depth of penetration of the spheres was measured with a micrometer depth gage. Six measurements were made for each test and the average value was determined for θ_o calculation. After depth measurement, the bin was weighed for void ratio determination.

A uniform, well-rounded, standard sand (20-30 mesh size) and a crushed Turkish emery* were used for the tests. Turkish emery has a similar grain

*Supplied by Hamilton Emery and Corundum Company, Chester, Mass.

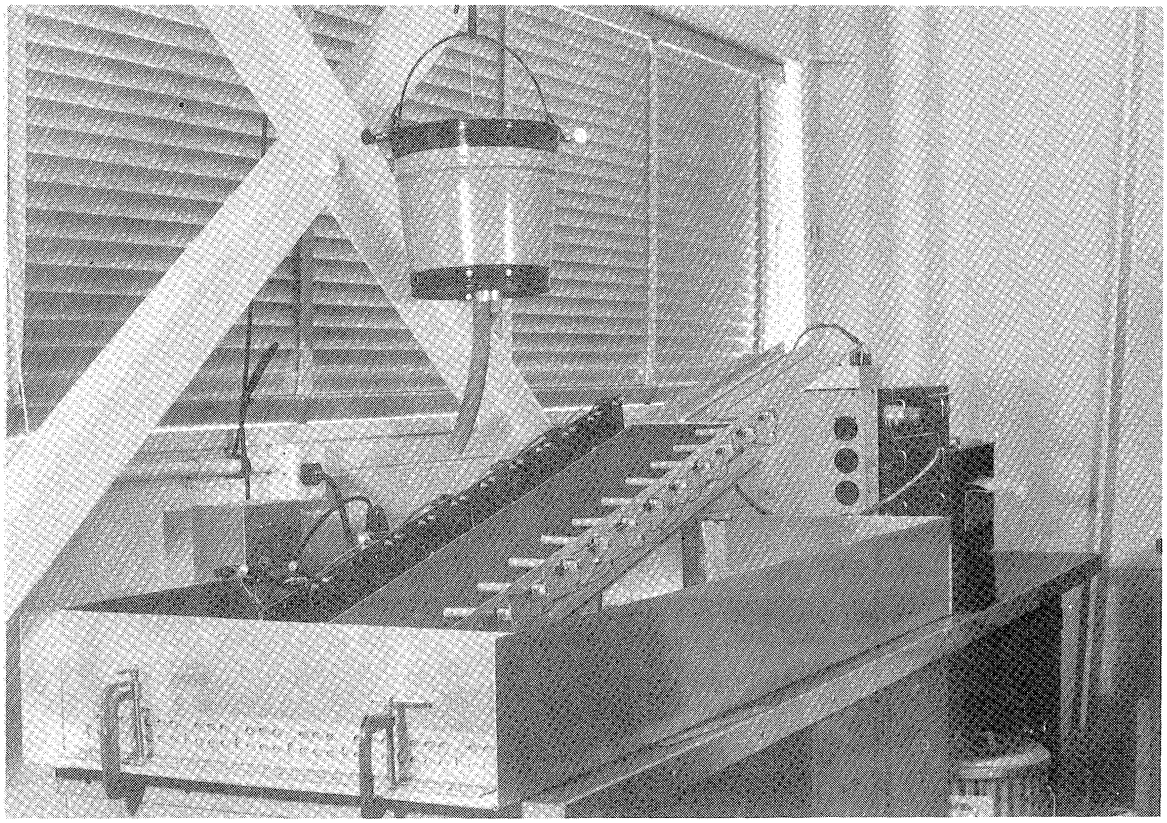

Figure 3. General view of experimental setup.

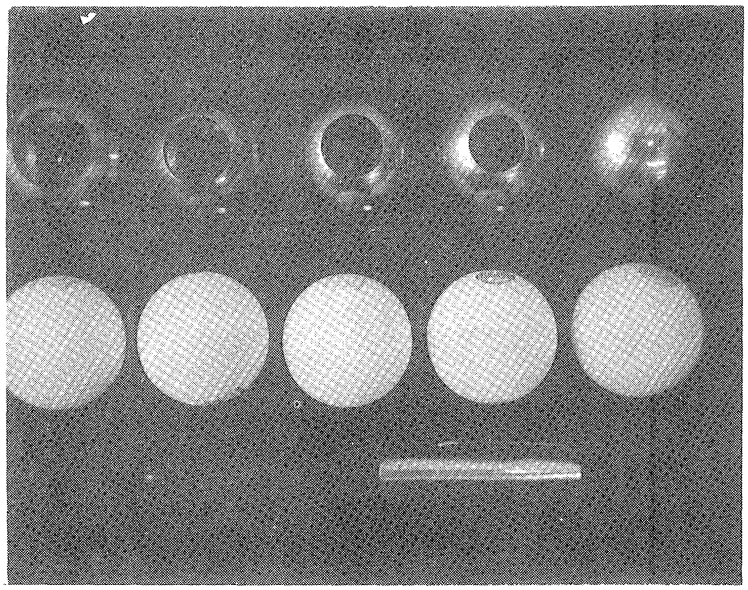

Figure 4. Experimental spheres before and after encapsulation in table tennis balls.

size distribution as Ottawa sand, but it is much more angular and has a higher specific gravity (G_S = 3.8). The composition and some of the physical properties of Turkish emery are given in Table I. Test results for Ottawa sand and the Turkish emery are tabulated in Tables II and III respectively. The results are also plotted in Figures 6 and 7 in terms of the functional relationship expressed in Eq. (10).

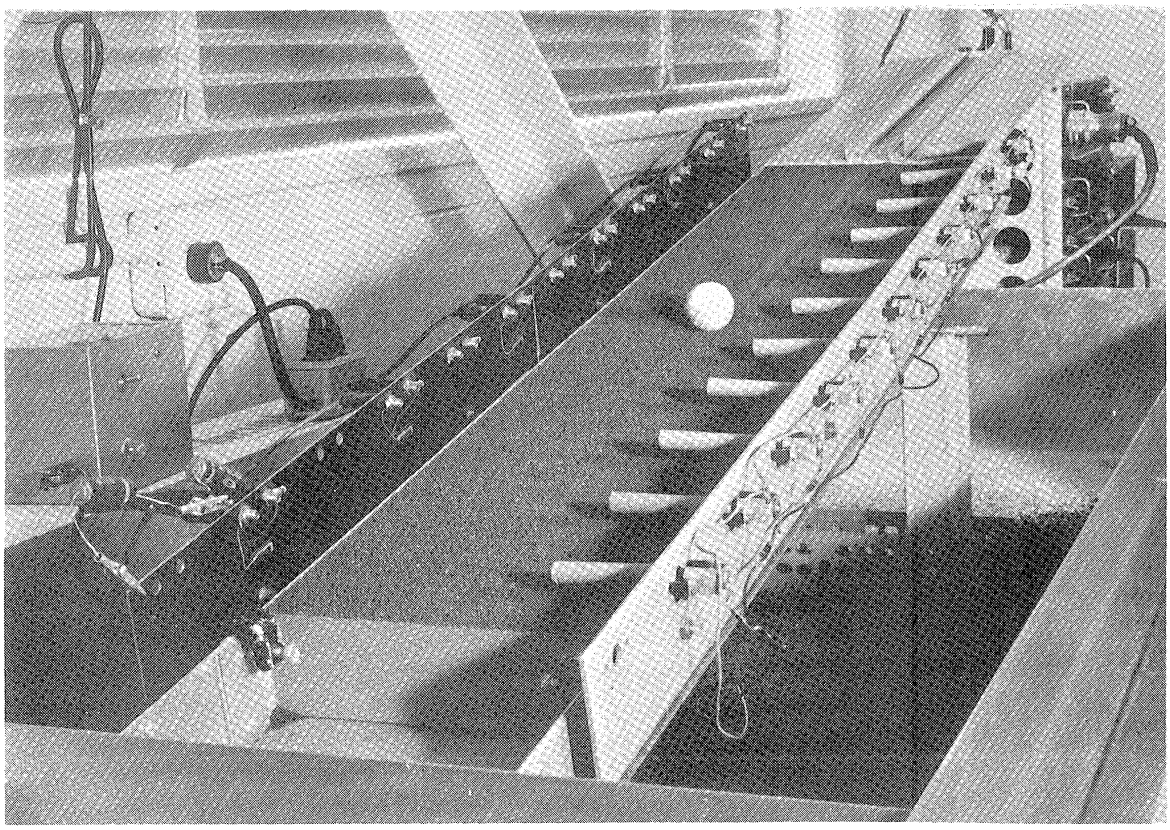

Figure 5. A rolling sphere on the inclined sand bin.

TABLE I

PHYSICAL PROPERTIES OF TURKISH EMERY

Specific Gravity:	3.8
Particle Shape:	Sharp, angular
Color:	Dark gray

Chemical Analyses		Grain Size Distribution	
Minerals	%	Mesh Size	%
Al_2O_3	67.35	16	0
SiO_2	3.5	20	15
Fe_3O_4	24.5	25	44
TiO_2	3.5	30	39
MgO	.14	35	2
CaO	.18	40	Trace
MnO	.07		
Ignition Loss	.76		

TABLE II

TEST DATA AND RESULTS FOR OTTAWA SAND

Test No.	γ_b (gm/cm^3)	γ_s (gm/cm^3)	ϕ (deg)	$\frac{1-\sin\phi}{1+\sin\phi}\left[\frac{\gamma_b}{\gamma_s}\right]^{1/2}$	b (cm)	θ_o
1	0.94	1.78	36.9	0.182	0.98	0.0828
6		1.78	36.6	0.184	0.99	0.0833
7		1.76	35.4	0.195	0.97	0.0817
12		1.73	33.8	0.211	1.14	0.0973
20		1.74	34.3	0.205	1.04	0.0883
2	1.23	1.79	37.1	0.206	1.08	0.0916
8		1.76	35.6	0.221	1.12	0.0950
14		1.72	33.3	0.246	1.32	0.1127
21		1.74	34.3	0.235	1.23	0.1045
3	1.76	1.78	36.9	0.249	1.23	0.1045
9		1.74	34.3	0.281	1.47	0.1267
15		1.68	31.5	0.321	1.59	0.1367
17		1.76	35.4	0.266	1.37	0.1171
22		1.73	33.8	0.288	1.47	0.1260
23		1.75	35.0	0.272	1.44	0.1235
4	2.26	1.80	37.7	0.270	1.39	0.1189
10		1.74	34.3	0.319	1.60	0.1378
16		1.68	31.4	0.365	1.86	0.1622
18		1.76	35.5	0.301	1.57	0.1355
5	2.82	1.78	36.9	0.315	1.68	0.1456
11		1.74	34.3	0.356	1.85	0.1618
19		1.76	35.4	0.337	1.74	0.1510

TABLE III

TEST DATA AND RESULTS FOR TURKISH EMERY

Test No.	γ_b (gm/cm^3)	γ_s (gm/cm^3)	ϕ (deg)	$\frac{1-\sin\phi}{1+\sin\phi}\left[\frac{\gamma_b}{\gamma_s}\right]^{1/2}$	b (cm)	θ_o
9	0.94	2.03	38.6	0.157	1.12	0.0950
14		1.98	35.1	0.185	1.27	0.1078
6	1.23	2.13	44.8	0.140	1.07	0.0911
10		2.06	40.0	0.167	1.16	0.0983
15		1.96	34.1	0.220	1.38	0.1178
3	1.76	2.02	37.9	0.225	1.26	0.1078
8		2.15	45.9	0.161	1.08	0.0915
11		2.06	40.0	0.202	1.29	0.1092
16		1.97	34.4	0.264	1.41	0.1206
18		2.04	39.3	0.208	1.27	0.1082
2	2.26	2.09	42.0	0.214	1.18	0.1005
4		2.26	51.8	0.133	0.95	0.0806
5		2.21	49.0	0.155	0.97	0.0820
12		2.06	40.0	0.229	1.30	0.1110
17		1.99	35.8	0.280	1.52	0.1306
1	2.82	2.24	51.1	0.153	1.03	0.0870
7		2.16	46.2	0.201	1.15	0.0978
13		2.06	40.0	0.254	1.43	0.1221

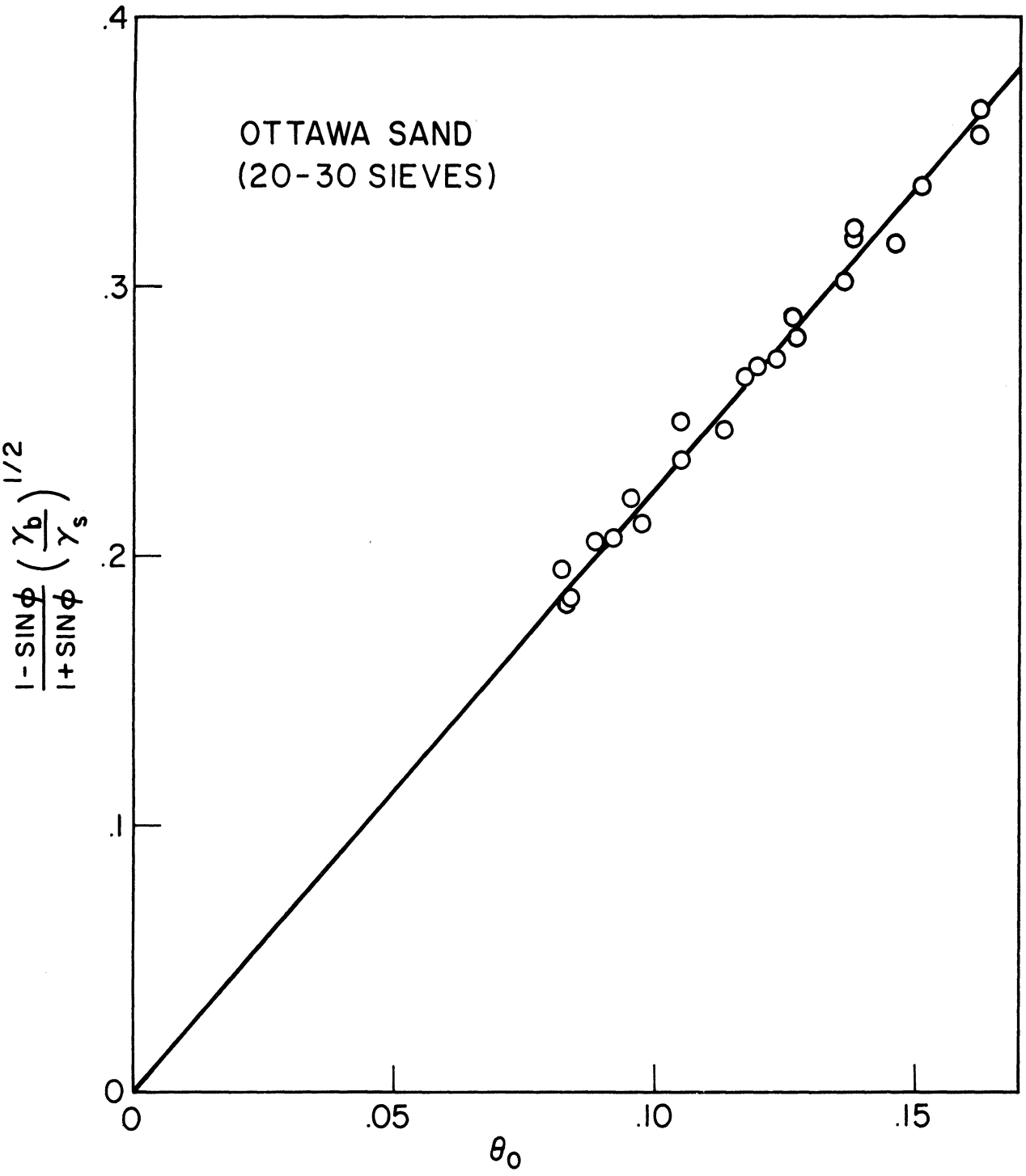

Figure 6. Experimental relation between two parametric functions for Ottawa sand.

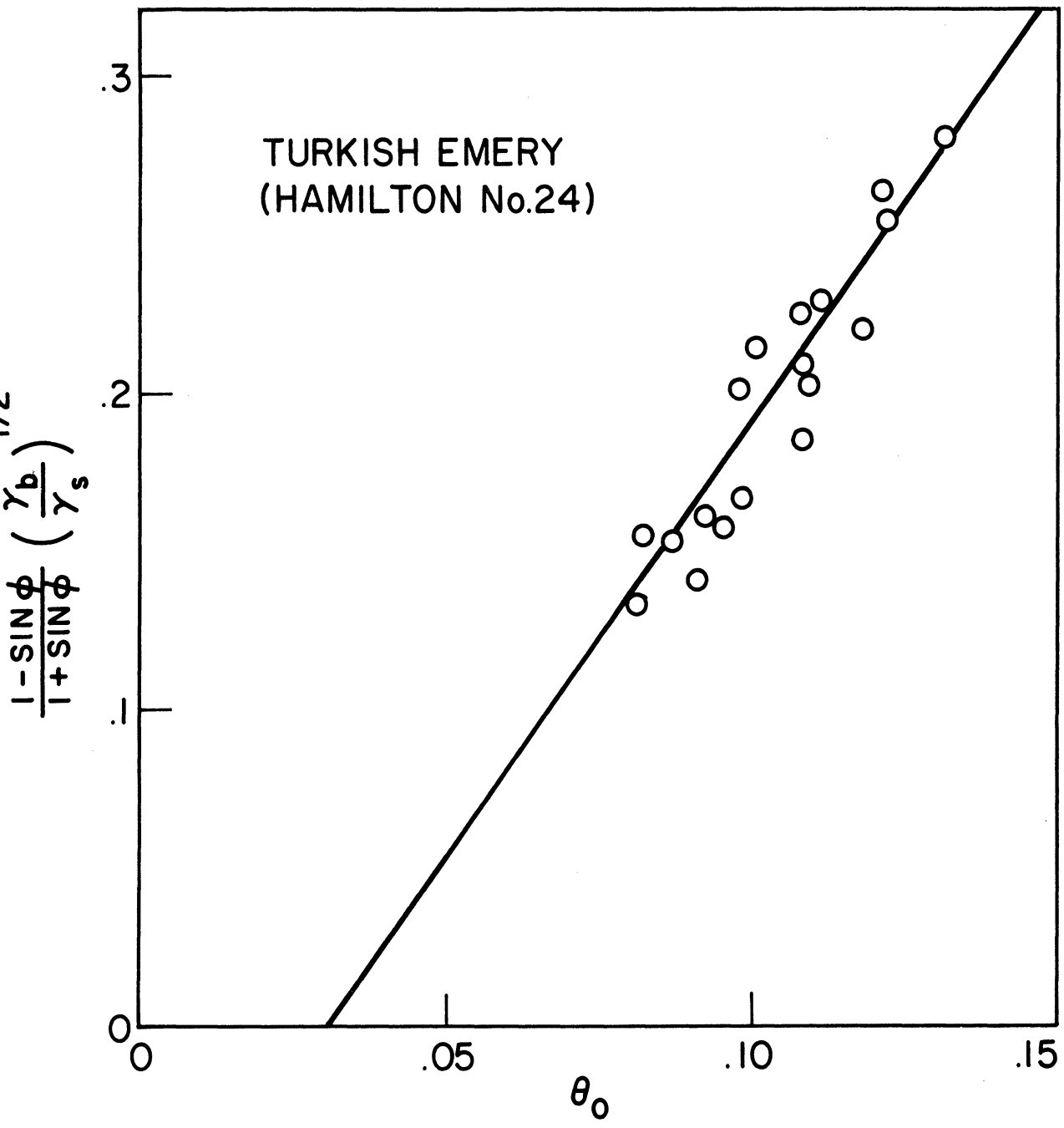

Figure 7. Experimental relation between two parametric functions for Turkish emery.

DISCUSSION AND CONCLUSIONS

A functional relationship between soil deformation and properties of the soil and sphere as expressed by Eq. (10) appears reasonably well established. The results shown in Figures 6 and 7 indicate relatively good agreement between experiment and theory. The hypothesis of "bulldozing" action by a rolling sphere combined with a "buoyancy" effect from the displaced soil seems a reasonable analytical approach to the problem.

The experiments with Turkish emery show some scattering of data points and a small deviation from theoretical prediction. The scatter is probably caused by experimental difficulty in obtaining an accurate depth measurement because of the extreme angularity of emery particles. The depth was measured down to the tops or asperities of the particle grains protruding above some average surface defined by their centers. The deviation of the experimental curve, viz., the fact it does not pass through the origin, may be caused by preferred particle orientation or alignment in the track or groove as opposed to a random orientation in the undisturbed, deposited material. Because of extreme angularity and particle asymmetry, the particles may have reoriented themselves from a random orientation to a preferred alignment after the material was subjected to the loading of a moving sphere. This would tend to make the measured depth of penetration higher than it actually was. A very small, but consistent error in depth measurement could shift the curve to the right and produce an intercept on the abcissa as shown in Figure 7.

Some possible applications or extensions of the present study are worth noting. For example, if the properties of a soil are known then it might be possible to predict the amount of plastic deformation from a given wheel load. Conversely, from analysis of the deformation produced by a rolling object of known density it might be possible to predict the shear strength properties of the surface on which it rolls. This latter possibility is of some interest in regard to the problem of predicting the properties of the moon's surface.

In recent years much attention has been directed to the determination of the mechanical properties of lunar soil. Attempts have been made to estimate the properties of the lunar surface from tracks formed by rolling boulders or fragments. Nordmeyer and Mason[6] estimated soil parameters from boulder track dimensions by using Terzaghi's bearing capacity equation. The method of analysis developed in the present study could also be adapted in a similar manner. For example, if the density of the lunar boulder or rock fragment can be determined, the soil strength could then be predicted from track measurements. On the other hand, if the lunar soil properties could be described, one might be able to determine the boulder's density. Some interesting examples of this type of analysis using Figure 6 and lunar data available in the literature are given below

Soil properties interpreted by Nordmeyer and Mason from the Surveyor I Mission Report are

$$\phi = 33°$$

$$c = 0.05 \text{ psi}$$

$$\gamma_s = 0.25 \text{ g/cm}^3 \text{ (under lunar gravity)}$$

A track 5 meters wide formed by a boulder 9 meters across was observed from Orbitor II. This is equivalent to a dimensionless track parameter

$$\theta_o = 0.187$$

Ignoring c, we obtain from the slope of the curve in Figure 6 the following relationship

$$\frac{1-\sin\phi}{1+\sin\phi}\left[\frac{\gamma_b}{\gamma_s}\right]^{1/2} = 0.42$$

Substituting the values for ϕ and γ_s given by Nordmeyer and Mason we calculate a boulder density as follows

$$\frac{1-\sin 33°}{1+\sin 33°}\left[\frac{\gamma_b}{0.25x6}\right]^{1/2} = 0.42$$

$$\gamma_b = 3.05 \text{ gm/cm}^3$$

This density is quite reasonable, particularly if the lunar surface is composed of a basalt-like material.

Surveyor V mission[7] reported some tracks, a millimeter to a few millimeters deep formed by fragments no more than 2 cm across. If a fragment of 2 cm across with a track of 2 mm deep is chosen, and one assumes a fragment density of 3 gm/cm^3, a soil bulk density of 1.43 gm/cm^3, or 0.238 gm/cm^3 under lunar gravity, would be predicted using the analysis previously described. It is important, of course, to keep in mind the boundary conditions for which this analysis was developed and to note that lunar soil properties and environment are not the same as those on earth. Nevertheless, the analytical approach appears promising and should be pursued further.

ACKNOWLEDGMENT

The authors wish to express their appreciation to Professor D. H. Gray for his helpful suggestions during this work and for his review of the manuscript.

REFERENCES

1. Bekker, M. G., Theory of Land Locomotion, The University of Michigan Press, 1956.

2. Vey, E., and Nelson, J. D., "Engineering Properties of Simulated Lunar Soils," Journal of the Soil Mechanics and Foundations Division, Proc. ASCE, 91 No. SM1, Jan., 1965.

3. Turkevich, A. L. et al., "Chemical Analysis of the Moon at the Surveyor V Landing Site," Surveyor V Reports, Science, Nov. 3, 1967.

4. Mitchell, J. K., "Current Lunar Soil Research," Journal of the Soil Mechanics and Foundations Division, Proc. ASCE, 90, No. SM3, May, 1964.

5. Langhaar, H. L., Dimensional Analysis and Theory of Models, John Wiley and Sons, Inc., 1951.

6. Nordmeyer, E. F., and Mason, C. C., "Lunar Surface Mechanical Properties Derived from Track Left by Nine Meter Boulder," NASA-MSC internal Note No. 67-TH-1, Feb., 1967.

7. Shoemaker, E. M., et al., "Television Pictures," Surveyor V Reports, Science, Nov. 3, 1967.

APPENDIX I

NOTATION

e = void ratio of soil
K, K_1, K_2 = non-dimensional constants
k_i = exponents of variables
p = non-dimensional coefficient of earth pressure
R = the component of passive Rankine force in the direction of sphere motion (gm)
r = radius of the sphere (cm)
W = weight of the sphere (gm)
w = weight of granular material displaced by the portion of the sphere lying below the original surface (gm)
α = angle of inclined surface (degree)
θ_o = angle of half of the groove cross section measured at the center of sphere (π)
γ_b = density of the sphere (gm/cm^3)
γ_s = density of granular meterial (gm/cm^3)
ϕ = angle of internal friction (degree)
σ_1 = major principal stress in the passive Rankine state
π^* = product of variables

APPENDIX II

DERIVATION OF THE WEIGHT OF MATERIAL DISPLACED BY A SPHERE

Assume the granular material displaced by an indenting sphere has a volume in the form of a spherical cap. From Figure 8(a),

$$dV = \pi(r\sin\theta)^2 dh$$

$$= \pi r^3 \sin^3\theta \, d\theta$$

$$V = \int dV = \pi r^3 \int_0^{\theta_o} \sin^3\theta \, d\theta$$

$$= \frac{4}{3}\pi r^3 \left[\frac{1}{2} - \frac{3}{4}\cos\theta_o + \frac{1}{4}\cos^3\theta_o\right]$$

$$w = V\gamma_s = \frac{4}{3}\pi r^3 \gamma_s \left[\frac{1}{2} - \frac{3}{4}\cos\theta_o + \frac{1}{4}\cos^3\theta_o\right]$$

For small θ_o,

$$\frac{1}{2} - \frac{3}{4}\cos\theta_o + \frac{1}{4}\cos^3\theta_o$$

$$= \frac{1}{2} - \frac{3}{4}\left(1 - \frac{1}{2}\theta_o^2\right) + \frac{1}{4}\left(1 - \frac{1}{2}\theta_o^2\right)^3$$

$$= \frac{3}{16}\theta_o^4 - \frac{1}{32}\theta_o^6 \approx \frac{3}{16}\theta_o^4$$

$$\therefore w = \frac{\pi}{4} r^3 \gamma_s \theta_o^4$$

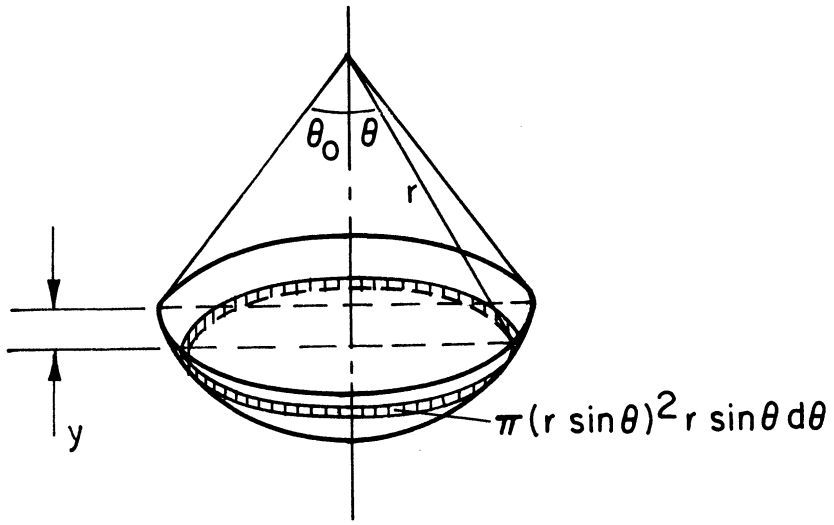

Figure 8(a). Diagram of volume of soil displaced by indenting sphere.

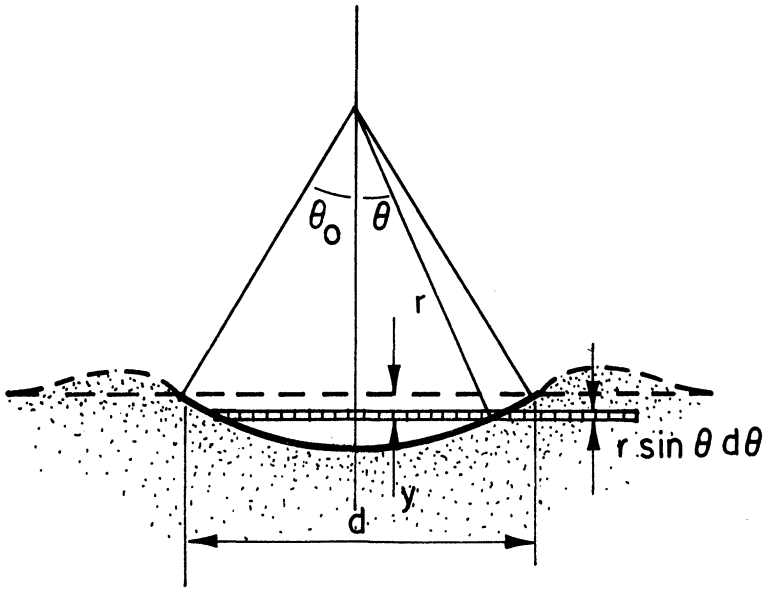

Figure 8(b). Cross section of sphere's track perpendicular to the inclined surface.

APPENDIX III

DERIVATION OF PASSIVE RANKINE FORCE
IN THE DIRECTION PARALLEL TO THE INCLINED SURFACE

1. MAJOR PRINCIPAL STRESS σ_1 IN PASSIVE RANKINE STATE

From Figure 9, let $\overline{OA} = p\gamma_s z$

$$\overline{AC} = \overline{AB},\ p\gamma_s z \sin\phi = \gamma_s z\sqrt{\sin^2\alpha + (p - \cos\alpha)^2}$$

$$p = \frac{\cos\alpha + \sqrt{\sin^2\phi - \sin^2\alpha}}{\cos^2\phi}$$

$$\sigma_1 = \overline{OD} = \gamma_s z\,(p + r) = \gamma_s zp\,(1 + \sin\phi)$$

$$\sigma_1 = \left[\frac{\cos\alpha + \sqrt{\sin^2\phi - \sin^2\alpha}}{1 - \sin\phi}\right]\gamma_s z$$

2. COMPONENT OF PASSIVE RANKINE FORCE IN THE DIRECTION OF INCLINED SURFACE

For moderate slopes, the value of the principal stress can be sutstituted for the normal stress on yz plane (Figure 1).

$$\sigma_1 = \left[\frac{\cos\alpha + \sqrt{\sin^2\phi - \sin^2\alpha}}{1 - \sin\phi}\right]\gamma_s y/\cos\alpha$$

From Figure 8(b),

$$R = 2\,\sigma_1 \int_o^{\theta_o} r^2 \sin^2\theta\, d\theta$$

$$= 2\left(\frac{\sigma_1}{y}\right) r^3 \int_o^{\theta_o} \sin^2\theta\,(\cos\theta - \cos\theta_o)\, d\theta$$

$$R = 2r^3\gamma_s \frac{1 + \sqrt{1 - (\cos\phi/\cos\alpha)^2}}{1 - \sin\phi}\left(\frac{1}{2}\sin\theta_o - \frac{1}{2}\theta_o\cos\theta_o - \frac{1}{6}\sin^3\theta_o\right)$$

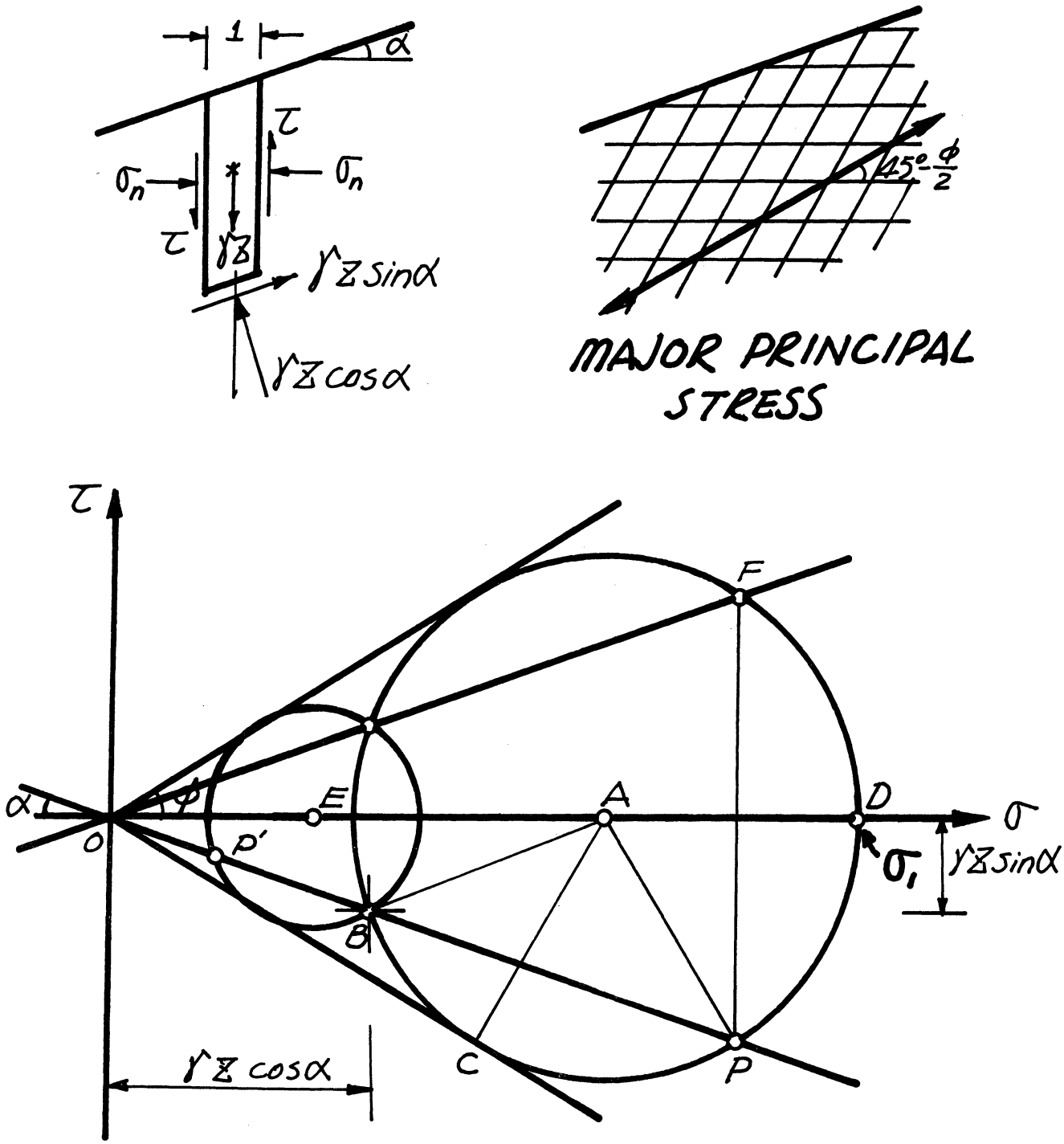

Figure 9. State of stress for a cohesionless mass with an inclined surface.

For the condition of the slope angle α smaller than the angle of repose of loose sand,

$$\cos \alpha \approx 1$$

Then,

$$R = 2r^3 \gamma_s \frac{1+\sin \phi}{1-\sin \phi} \left(\frac{1}{2} \sin \theta_o - \frac{1}{2} \theta_o \cos \theta_o - \frac{1}{6} \sin^3 \theta_o\right)$$

For small θ_o,

$$\frac{1}{2} \sin \theta_o - \frac{1}{2} \theta_o \cos \theta_o - \frac{1}{6} \sin^3 \theta_o$$

$$= \frac{1}{2} \left(\theta_o - \frac{\theta_o^3}{6}\right) - \frac{1}{2} \theta_o \left(1 - \frac{1}{2} \theta_o^2\right) - \frac{1}{6} \left(\theta_o - \frac{1}{6} \theta_o^3\right)^3$$

$$= \frac{1}{12} \theta_o^5 - \frac{1}{72} \theta_o^7 + \frac{1}{1296} \theta_o^9$$

$$\approx \frac{1}{12} \theta_o^5$$

$$R = \frac{1}{6} r^3 \gamma_s \theta_o^5 \left[\frac{1+\sin \phi}{1-\sin \phi}\right]$$